

# Redox Chemistry of Trinuclear Complexes possessing a Hexathiolatomolybdate(IV) Core: *in situ* Syntheses, Characterization and Geometry Optimization†

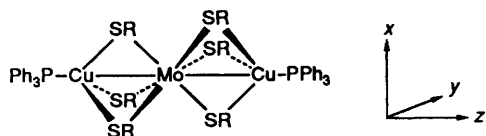
Heinz-Bernhard Kraatz,<sup>a</sup> P. Michael Boorman,<sup>a,\*</sup> A. Scott Hinman,<sup>a</sup> Tom Ziegler,<sup>a</sup> David Collison<sup>b</sup> and Frank E. Mabbs<sup>b</sup>

<sup>a</sup> Department of Chemistry, University of Calgary, Calgary, Alberta T2N 1N4, Canada

<sup>b</sup> Department of Chemistry, Manchester University, Manchester M13 9PL, UK

The trinuclear heterobimetallic clusters  $[(\text{Ph}_3\text{P})\text{Cu}(\mu\text{-SR})_3\text{Mo}(\mu\text{-SR})_3\text{Cu}(\text{PPh}_3)]$  ( $\text{R} = \text{C}_6\text{H}_4\text{Me-4}$  **2**,  $\text{C}_6\text{H}_4\text{F-4}$  **3**,  $\text{C}_6\text{H}_4\text{Cl-4}$  **4** or  $\text{C}_6\text{H}_4\text{Br-4}$  **5**) have been found to undergo reversible one-electron reductions. The reduction potential is sensitive to the *para* substituent on the thiolate and has been correlated with the electron-donating properties of the substituent. In addition, **2** undergoes a reversible one-electron oxidation. According to EPR measurements, the oxidation of **2** is molybdenum-based. Geometry optimizations based on density functional theory of the oxidized and reduced model cluster  $[(\text{H}_3\text{P})\text{Cu}(\mu\text{-SH})_3\text{Mo}(\mu\text{-SH})_3\text{Cu}(\text{PH}_3)]$ , assuming retention of the  $D_3$  point-group symmetry, have shown that both redox processes will lead to an elongation of the Mo–Cu vector. Reduction of the central molybdenum fragment will decrease the strength of the Cu to Mo donor bond. Oxidation of the central molybdenum fragment will result in a decrease of electrostatic interaction with the  $[(\text{H}_3\text{P})\text{CuCu}(\text{PH}_3)]^{2+}$  fragment. The reaction of **2** with  $\text{NOBF}_4$  results in oxidation of the cluster. The IR spectrum of the diamagnetic reaction product shows a band at  $1657\text{ cm}^{-1}$  suggesting the presence of co-ordinated  $\text{NO}^-$ . Further evidence is provided by  $^{14}\text{N}$  NMR spectroscopy. The reactions of **2** and **5** with arenediazonium salts result in degradation of the clusters, with the liberation of organic sulfides and disulfides, suggesting the involvement of free thiyl radicals.

We recently described<sup>1,2</sup> the synthesis and characterization of the paramagnetic heterobimetallic clusters  $[(\text{Ph}_3\text{P})\text{Cu}(\mu\text{-EC}_6\text{H}_4\text{Me-4})_3\text{W}(\mu\text{-EC}_6\text{H}_4\text{Me-4})_3\text{Cu}(\text{PPh}_3)]$  ( $\text{E} = \text{S}$  **1** or  $\text{Se}$  **6**) and  $[(\text{Ph}_3\text{P})\text{Cu}(\mu\text{-SR})_3\text{Mo}(\mu\text{-SR})_3\text{Cu}(\text{PPh}_3)]$  ( $\text{R} = \text{C}_6\text{H}_4\text{Me-4}$  **2**,  $\text{C}_6\text{H}_4\text{F-4}$  **3**,  $\text{C}_6\text{H}_4\text{Cl-4}$  **4**, or  $\text{C}_6\text{H}_4\text{Br-4}$  **5**). According to



calculations based on density functional theory (DFT) performed on models of **1** and **2** the cluster contains two unpaired electrons, which are situated in a set of doubly degenerate mainly central-metal based orbitals (41% M  $d_{x^2-y^2}$  + 21% M  $d_{yz}$  and 41% M  $d_{xy}$  + 21% M  $d_{xz}$ ). This suggests that any redox chemistry of the clusters will take place on the central metal. Metal-based redox processes are of fundamental importance to redox enzymes.<sup>3</sup> In the case of molybdenum, this has stimulated extensive research focusing on the modelling of reactions of nitrogen-containing molecules with certain enzymes.<sup>4</sup> In particular the co-ordination chemistry of sulfur-ligated molybdenum complexes with small nitrogen-containing molecules may well serve as models to gain an understanding of some of the fundamental steps in enzymatic processes. There is precedence for the activation of small nitrogen-containing molecules by sulfur-ligated molybdenum complexes. For example, Sellmann and co-workers<sup>5</sup> have successfully reduced  $\text{NO}$  to  $\text{NH}_2\text{OH}$  on a partially sulfur-ligated molybdenum(II)

centre, possibly a key step in the enzymatic conversion of  $\text{NO}_3^-$  into  $\text{NH}_3$ . Catalytic conversion of  $\text{H}_2\text{N-NH}_2$  into  $\text{NH}_3$ , thought of as a key step in the fixation of dinitrogen, is achieved by the binuclear dimolybdenum(IV) complex  $[\text{Mo}_2\text{Cl}_4(2\text{-SC}_5\text{H}_3\text{N-3-SiMe}_3)_2(\mu\text{-S}_2)(\mu\text{-2-SC}_5\text{H}_3\text{NH-3-SiMe}_3)]$ .<sup>6</sup> In this context, the redox chemistry of complexes containing the novel hexathiolatomolybdate core is of particular interest.

In this study we report the electrochemical syntheses and spectroscopic characterization of cluster cations and anions derived from the parent complexes **2-5**. The geometries of the model clusters  $[(\text{H}_3\text{P})\text{Cu}(\mu\text{-SH})_3\text{Mo}(\mu\text{-SH})_3\text{Cu}(\text{PH}_3)]^{7+}$  and  $[(\text{H}_3\text{P})\text{Cu}(\mu\text{-SH})_3\text{Mo}(\mu\text{-SH})_3\text{Cu}(\text{PH}_3)]^{7-}$  were calculated using density functional theory. In addition we report the oxidation of **2** with the small nitrogen-containing ions  $\text{NO}^+$  and  $\text{RN}_2^+$  ( $\text{R} = \text{C}_6\text{H}_4\text{NO}_2\text{-4}$  or  $\text{C}_6\text{H}_4\text{OMe-4}$ ) and the spectroscopic characterization of some of the products.

## Results and Discussion

**Electrochemistry.**—A summary of the cyclic voltammetric data is given in Table 1. Complexes **2-5** exhibit a reversible one-electron reduction wave. The reduced species seem to be stable on the voltammetric time-scale. The ratios of cathodic to anodic peak currents,  $i_{pc}/i_{pa}$ , are close to unity and independent of the scan rate, indicating a reversible process. The separation of anodic and cathodic peak currents is close to the reversible limit for a one-electron process (59 mV). In addition to the reversible one-electron reduction, **2** shows a reversible one-electron oxidation wave at 0.23 V *versus* the saturated calomel electrode (SCE). The cyclic voltammogram for **2** in  $\text{CH}_2\text{Cl}_2$  at a sweep rate of  $100\text{ mV s}^{-1}$  showing the two reversible processes is in Fig. 1. In addition, **2** exhibits an irreversible oxidation wave at 1.0 V (scan rate  $100\text{ mV s}^{-1}$ ). The clusters **3-5** show only irreversible oxidation waves (see below).

The reduction potential is sensitive to the *para* substituent on

† Supplementary data available (No. SUP 56940, 2 pp.): NMR spectra. See Instructions for Authors, *J. Chem. Soc., Dalton Trans.*, 1993, Issue 1, pp. xxiii–xxviii.

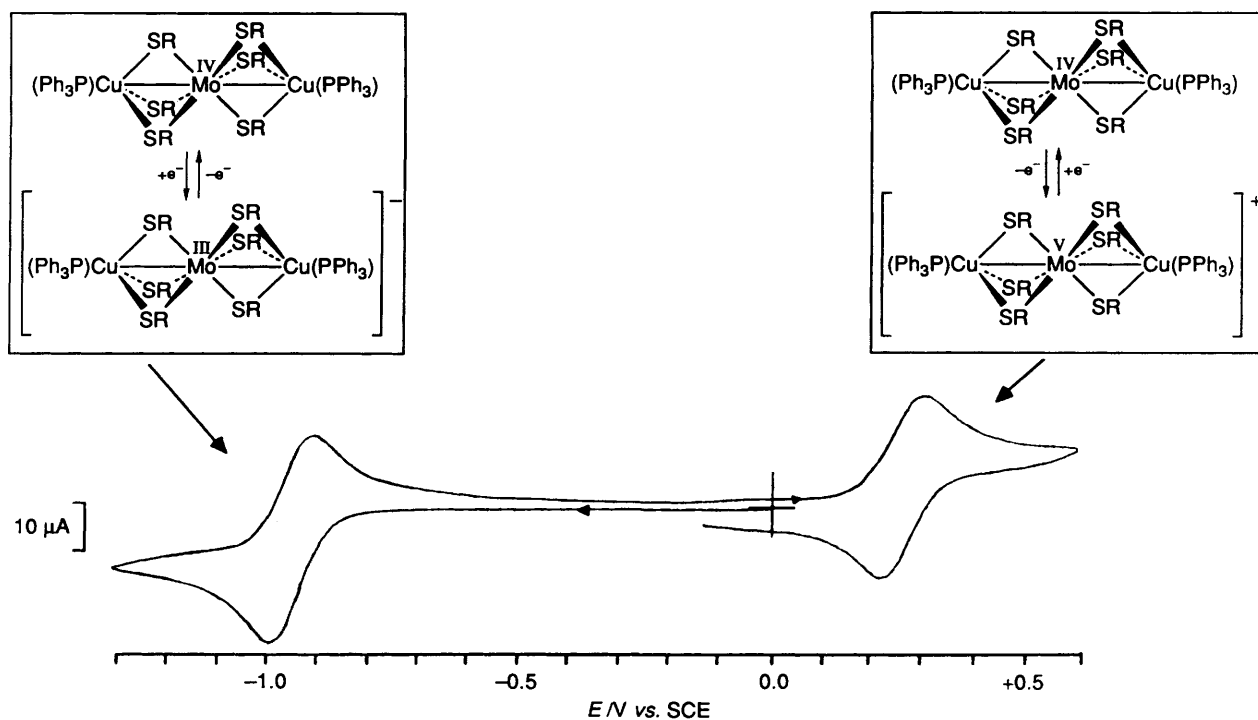


Fig. 1 Cyclic voltammogram of complex **2** in  $0.1 \text{ mol dm}^{-3} \text{ NBu}_4\text{ClO}_4\text{-CH}_2\text{Cl}_2$  at  $100 \text{ mV s}^{-1}$ ;  $\text{R} = \text{C}_6\text{H}_4\text{Me-}p$

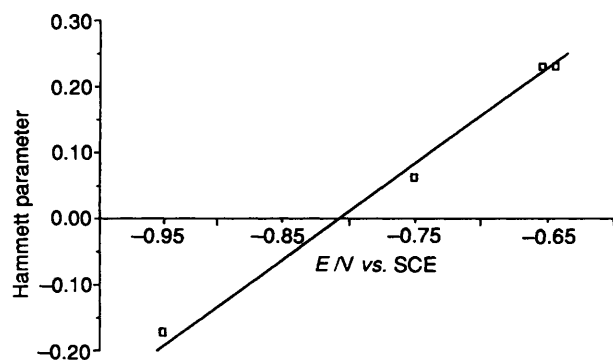


Fig. 2 Plot of Hammett function versus the reduction potential for complexes **2-5**

Table 1 Cyclic voltammetry data for the clusters  $[(\text{Ph}_3\text{P})\text{Cu}(\mu\text{-SR})_3\text{Mo}(\mu\text{-SR})_3\text{Cu}(\text{PPh}_3)]$  **2-5** in  $\text{CH}_2\text{Cl}_2$  with  $0.1 \text{ mol dm}^{-3} \text{ NBu}_4\text{PF}_6$  as supporting electrolyte. All potentials are given in V versus SCE

Compound	$\text{Mo}^{\text{IV}} \rightarrow \text{Mo}^{\text{III}}$		$E_{\text{ox}}$	Hammett function
	$E_{\text{r}1/2}$	$i_{\text{pc}}/i_{\text{pa}}$		
<b>2</b>	-0.95	1.01	0.23 <sup>a</sup>	-0.17
<b>3</b>	-0.75	0.95	0.58 <sup>b</sup>	0.06
<b>4</b>	-0.65	0.98	0.60 <sup>b</sup>	0.23
<b>5</b>	-0.66	0.97	0.62 <sup>b</sup>	0.23

<sup>a</sup> Reversible one-electron oxidation, half-wave potential,  $i_{\text{pc}}/i_{\text{pa}} = 0.95$ .  
<sup>b</sup> Irreversible oxidation, value is peak potential at  $100 \text{ mV s}^{-1}$ .

the arenethiolate. As this becomes more electron donating the reduction of the cluster becomes more difficult. The Hammett function  $\sigma$  is considered to be a measure of the electron-donating ability of a substituent.<sup>7</sup> A linear correlation between the reduction potential and the electron-donating properties of the *para* substituent is shown as a plot of  $E_{\text{red}}$  versus the Hammett function  $\sigma$  for the 0/1 - couple in Fig. 2. Similar linear relationships were observed for the oxomolybdenum system

$[\text{MoO}(\text{SR})_4]^-$ ,<sup>8</sup> for the well known<sup>9</sup> cubanes  $[\text{Fe}_4\text{S}_4(\text{SC}_6\text{H}_4\text{-X-4})_4]^{2-3-}$  and for thiolate-bridged manganese binuclear systems.<sup>10</sup> In all three cases the nature of the substituent of the arenethiolate was seen as the main factor in determining the reduction potential of the complex. To influence greatly the redox behaviour, the orbital receiving the electrons should possess a significant contribution from the thiolate. In the case of the thiolate-bridged manganese binuclear systems, Fenske-Hall calculations<sup>10</sup> on the model compound  $[\text{Mn}_2(\mu\text{-SH})_2(\text{PH}_3)_2(\text{CO})_6]$  showed a 25% contribution from thiolate-based orbitals to the highest occupied molecular orbital (HOMO). Therefore, the oxidation of  $[\text{Mn}_2(\mu\text{-SH})_2(\text{PH}_3)_2(\text{CO})_6]$  shows the expected substituent influence.

The DFT calculations<sup>2</sup> on the model complex  $[(\text{H}_3\text{P})\text{Cu}(\mu\text{-SH})_3\text{Mo}(\mu\text{-SH})_3\text{Cu}(\text{PH}_3)]$  **7** showed that although the two singly occupied orbitals (SHOMOs) are mainly molybdenum-based, there is a 20.5% contribution from the bridging thiolate. An electron-donating substituent on the arenethiolate will raise the energy level of the SHOMOs thereby making the cluster more difficult to reduce. An electron-withdrawing substituent on the other hand will lower the energy levels of the SHOMOs and hence the reduction will be more facile. This is in accordance with the observed behaviour.

As stated above, the SHOMO is 79.5% molybdenum in character and hence redox processes would result in a change of oxidation state at the molybdenum centre. This means that upon reduction the central  $\text{Mo}^{\text{IV}}$  will be reduced to  $\text{Mo}^{\text{III}}$ . The oxidation will yield  $\text{Mo}^{\text{V}}$ .

**EPR Spectroscopy.**—To test our assumption we attempted bulk electrolysis of the clusters in  $\text{CH}_2\text{Cl}_2$  and transferred the solution containing the reduced or oxidized complex into an EPR tube under argon and immediately cooled to 77 K. Unexpectedly, the reductions did not give clearly identifiable signals (see Experimental section).

Since the electrochemical oxidation of complex **2** is reversible on the cyclovoltammetric (CV) time-scale, chemical oxidation in toluene-acetone solution with ferrocenium hexafluorophosphate was used to generate  $2^+$ . The resulting solution was transferred into an EPR tube under argon and immediately

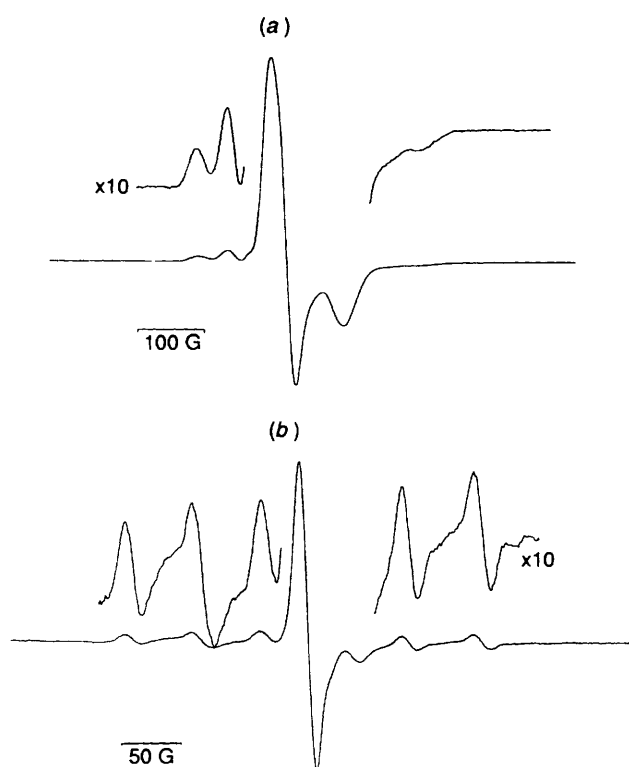


Fig. 3 The EPR spectra in toluene-acetone (1:1) of chemically generated complex  $2^+$ : (a) frozen solution, (b) liquid phase.  $G = 10^{-4}$  T

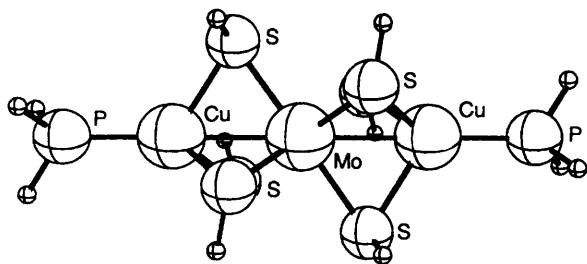


Fig. 4 Model complex 7

Table 2 Selected bond distances (in pm) and angles ( $^\circ$ ) for complex  $2$  (X-ray data, see ref. 2) and the optimized complexes  $7$ ,  $7^+$  and  $7^-$  (using AMOL, see ref. 11)

	Complex			
	7	7 <sup>+</sup>	7 <sup>-</sup>	2
Cu-Mo	263.0	267.6	270.2	269.1(1)
S-Mo	242.8	240.8	247.8	249.0(2)
P-Cu	219.1	219.7	217.6	220.9(4)
S-Cu	234.1	236.9	234.5	234.8(2)
S-Mo-Cu	55.0	55.2	53.8	53.7(1)
S-Cu-Mo	58.1	56.6	57.8	58.8(1)
S-Cu-P	121.9	123.4	122.2	121.2(1)
Cu-S-Mo	66.9	68.1	68.4	67.5(1)
S-Mo-S	90.3	90.7	88.7	88.6(1)
S-Cu-S	94.7	92.6	94.2	95.5(1)

cooled to 77 K. The frozen-solution spectrum of the product is shown in Fig. 3(a) and is indicative of a nearly axial EPR symmetry. The  $g$  values, assuming axial symmetry, are  $g_{\perp} = 1.984$  and  $g_{\parallel} = 1.936$ . There is clear indication of molybdenum hyperfine splitting. Warming to room temperature gives a signal centred at  $g = 1.967$  (a value close to the average from the frozen solution) with six satellites ( $A = 5.2$  mT) due to coupling

of the unpaired electron to  $^{95,97}\text{Mo}$  [Fig. 3(b)]. This clearly shows that the product of oxidation of the cluster is molybdenum-based and that there is no significant interaction of the unpaired electron with any other nuclei.

The chemical oxidation of clusters  $3-5$  with ferrocenium hexafluorophosphate did not allow the detection of the corresponding oxidized clusters ( $3^+-5^+$ ) by EPR spectroscopy. Instead a number of lines are present in the EPR spectrum, indicating the degradation of the oxidized complexes. In some spectra, lines due to Cu-based species were detected.

**Density Functional Study.**—The geometry of the trinuclear molybdenum-copper clusters has been idealized for the density functional calculations to possess  $D_3$  point-group symmetry, with the three-fold axis along the Mo-Cu vector, as shown in Fig. 4. The SHOMO is essentially a non-bonding orbital and hence structural changes will be minor in magnitude. All aryl substituents have been replaced by hydrogen atoms for ease of calculation. We have carried out geometry optimizations of  $[(\text{H}_3\text{P})\text{Cu}(\mu\text{-SH})_3\text{Mo}(\mu\text{-SH})_3\text{Cu}(\text{PH}_3)]$   $7$  and of its oxidized ( $7^+$ ) and reduced ( $7^-$ ) forms in  $D_3$  point-group symmetry with the aim of getting a qualitative picture of the geometrical changes that will take place upon oxidation and reduction of the complexes. As shown previously,<sup>2</sup> the major contributor to the overall bonding energy is the electrostatic attraction between the  $\text{Mo}(\text{SH})_6^{2-}$  and the  $[(\text{H}_3\text{P})\text{CuCu}(\text{PH}_3)]^{2+}$  fragments. A weak  $d^{10}\text{Cu}$  to  $d^2\text{Mo}$  donor bond is present. As seen above the redox processes are Mo-based. Hence the reduction was modelled by the interaction of  $\text{Mo}(\text{SH})_6^{3-}$  with  $[(\text{H}_3\text{P})\text{CuCu}(\text{PH}_3)]^{2+}$ , and the oxidation was modelled by allowing the interaction of  $\text{Mo}(\text{SH})_6^-$  with  $[(\text{H}_3\text{P})\text{CuCu}(\text{PH}_3)]^{2+}$ .

The results of the geometry optimizations are presented in Table 2 together with the bond lengths and angles of cluster  $2$  for comparison. Overall, it can be said that there is good agreement between the calculated bond lengths for  $7$  and the experimental values for  $2$  taking into account the crudity of our model. However, the differences will be largely steric in nature and understandably three arenethiolates in the bridge will lead to more steric repulsion than three sulfhydryl groups. Consequently, the Mo-S and Mo-Cu distances in our model will be slightly shorter than those observed for  $2$ .

Upon reduction, we observe a lengthening of the Mo-Cu bond from 263.0 to 270.2 pm. At the same time the Cu-P distance decreases by about 2 pm. This can be explained considering two opposing effects. As expected, the electrostatic interaction increases, since the interaction will be between a triply charged anion and a doubly charged cation. The exchange repulsion, that is the destabilizing four-electron two-orbital interaction, does not increase significantly. In contrast, the higher electron density on the central molybdenum will make any donation of electron density from the  $d^{10}$  copper more difficult, resulting in a lengthening of the Mo-Cu bond. The back-bonding interaction between the phosphine and the copper will be stronger and Cu-P bond distance will decrease.

The calculations on the oxidation of complex  $7$  show a lengthening of the Mo-Cu bond, the main reason being a significant decrease in the electrostatic interaction of the fragments. Enhanced Cu-Mo donor-acceptor interaction cannot compensate for the loss in electrostatic interaction. Reduced electron density on the copper will lead to a lengthening of the Cu-P bond.

The two non-bonding sulfur-sulfur distances in the neutral molecules  $7$  are 344.4 and 342.5 pm. It is interesting that upon oxidation these distances decrease to 342.6 and 338.4 pm, but this is more likely due to the reduced Mo-S distances rather than to attractive S...S interactions.

**Reaction of Complex 2 with  $\text{NOBF}_4$ .**—Assuming that  $\text{NO}^+$  would lead to a one-electron oxidation of complex  $2$  together

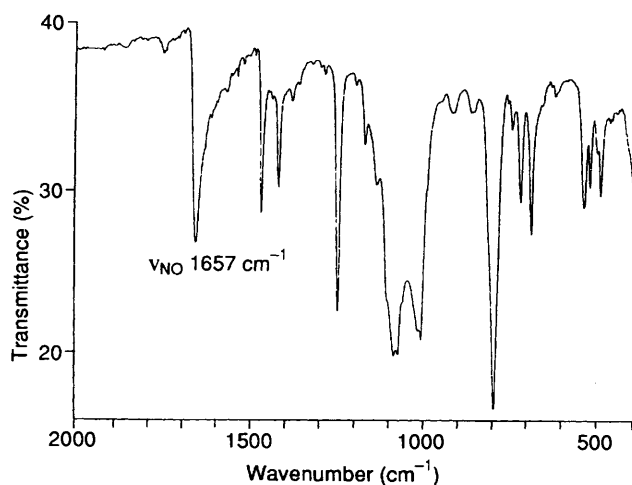


Fig. 5 The IR spectrum of the product of reaction of complex 2 with  $\text{NOBF}_4$  in  $\text{CH}_2\text{Cl}_2$  (KBr disk)

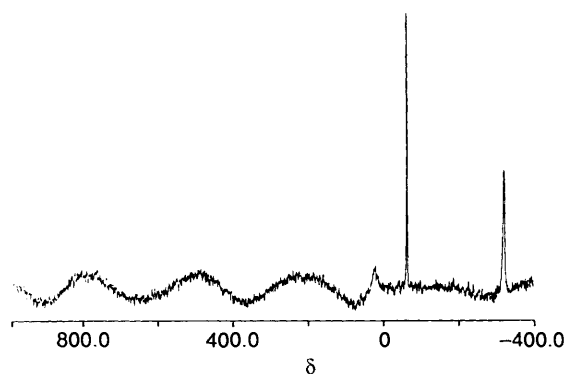
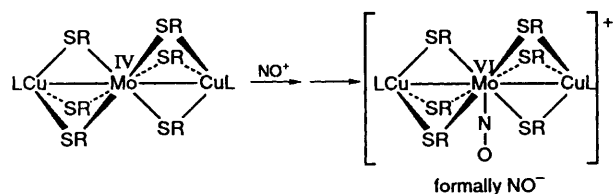


Fig. 6 The  $^{14}\text{N}$  NMR spectrum of the product of reaction of complex 2 with  $\text{NOBF}_4$  in  $\text{CH}_2\text{Cl}_2$  ( $\text{D}_2\text{O}$  insert)



Scheme 1

with the liberation of free NO gas,  $\text{NOBF}_4$  was used as the oxidizing agent. Upon addition of an excess of  $\text{NOBF}_4$  to a solution of **2** in either  $\text{CH}_2\text{Cl}_2$ , propionitrile, toluene or chlorobenzene at room temperature a slow colour change from purple to brown indicated reaction. Evaporation of the solvent yielded a brown oil, which was then washed with hexane. No organic decomposition products, such as disulfides or  $\text{PPh}_3$ , were detectable by gas chromatography–mass spectrometry (GC–MS). Attempts to crystallize this oil were unsuccessful. A change of anions did not result in a crystalline reaction product.

The  $^1\text{H}$  NMR spectrum of the diamagnetic brown oil indicated the presence of two different methyl environments in the product. The  $^{31}\text{P}$  NMR spectrum revealed four new signals. Judging from the disappearance of the signal due to the starting material ( $\delta -3.6$ ) the reaction was complete, leading to one major product ( $\delta +26.8$ ) and three minor products (about 7% by integration). The IR spectrum (Fig. 5) shows a new band at  $1657\text{ cm}^{-1}$  indicating the presence of a co-ordinated nitrosyl ligand. The low N–O stretching frequency suggests a strong back donation of electron density into the  $\pi^*$  orbital of NO. Similarly low N–O stretching frequencies have been observed for  $[\text{Mo}(\text{SPh})_4(\text{NO})]^-$  [ref. 12(a)] and  $[\text{Mo}(\text{NO})(\text{S}_2\text{CN}-$

$\text{Me}_2)_3]$ .<sup>12b</sup> Further evidence for the presence of a nitrogen-containing species was provided by the  $^{14}\text{N}$  NMR spectrum (Fig. 6) of the brown oil in  $\text{CH}_2\text{Cl}_2$  solution. Using dissolved  $\text{N}_2$  ( $\delta -71.5$  ppm, relative to  $\text{MeNO}_2$ ) as an internal standard, the spectrum reveals a broad intense signal at  $\delta -323.5$  with a linewidth of 170 Hz. The very broad resonance at about  $\delta +10$  is due to some residual  $\text{NO}^+$ . The high-field signal at  $\delta -323.5$  must be due to the main reaction product. There is no precedence for a nitrosyl signal at such a high field.<sup>13</sup> To our knowledge, the mononitrosyl complex  $[\text{Os}(\text{NH}_3)_5(\text{NO})]\text{Cl}_3$ , having a linear nitrosyl ligand, has the largest upfield shift reported to date.<sup>13f</sup> However, all shifts of nitrosyl complexes reported so far, bent or linear, are of complexes with an  $d(\text{M}) + \pi^*(\text{NO})$  electron count<sup>14a</sup> of six or higher. In contrast, for the proposed  $\text{MoCu}_2\text{-NO}$  cluster, the electron count will be two. In general, linear nitrosyls will be more shielded than bent nitrosyls.<sup>13c,f</sup> It has been pointed out that the M–N–O angle of transition-metal nitrosyl complexes containing  $\text{NO}^-$  can vary between 120 and  $180^\circ$ ;<sup>14</sup>  $\{\text{M}(\text{NO})\}^n$  complexes where  $n < 6$  will have a linear linkage.<sup>4a,d</sup> From the aforesaid, it can be concluded that the signal at this very unusual high field is most likely due to a co-ordinated linear  $\text{NO}^-$ . The linearity is probably the consequence of electronic effects and possibly steric crowding around the molybdenum centre.

To demonstrate that the oil is indeed ionic in nature, the conductance of a solution of it in propionitrile was measured at room temperature. The results show that the oil is dissociated in solution ( $\Lambda = 174\ \Omega^{-1}\text{ cm}^2\text{ mol}^{-1}$  for a  $1.8 \times 10^{-3}\text{ mol dm}^{-3}$  solution). Assuming that increasing concentration will increase the association and hence decrease the molar conductance, the value obtained is high for a 1:1 electrolyte. However, this value should only be interpreted as qualitative evidence of the ionic nature of the compound. Further evidence stems from the IR spectrum, which shows absorbances around  $1000\text{ cm}^{-1}$  that are distinctive for the  $\text{BF}_4^-$  anion<sup>15</sup> ( $\nu_3$  and  $\nu_4$  of  $\text{BF}_4^-$  are IR active and are observed at  $1016$  [ $\nu_3(\text{B}^{10}\text{F}_4^-)$ ],  $984$  [ $\nu_3(\text{B}^{11}\text{F}_4^-)$ ],  $529$  [ $\nu_4(\text{B}^{10}\text{F}_4^-)$ ] and  $524\text{ cm}^{-1}$  [ $\nu_4(\text{B}^{11}\text{F}_4^-)$ ]).

The evidence presented supports the reaction put forward in Scheme 1. The first step is the oxidation of the cluster by  $\text{NO}^+$ . Rather than leaving as NO gas, the resulting molybdenum(v) centre picks up NO to give a seven-co-ordinated  $\text{Mo}^{\text{V}}$ , followed by an internal electron transfer from the central  $\text{Mo}^{\text{V}}$  to the co-ordinated NO, formally making it  $\text{NO}^-$ , which renders the complex diamagnetic.

**Reaction of Complex 2 with  $[4\text{-O}_2\text{NC}_6\text{H}_4\text{N}_2][\text{BF}_4]$  and  $[4\text{-MeOC}_6\text{H}_4\text{N}_2][\text{BF}_4]$ .**—The redox behaviour of arenediazonium salts is well studied<sup>16</sup> and finds application in preparative organic synthesis for the introduction of halogens into the aromatic ring (Sandmeyer reaction)<sup>17</sup> and other radical reactions. Our aim was to use  $\text{RN}_2^+$  as a one-electron oxidizing agent. Oxidation would be expected to proceed with the formation of an aryl radical and the liberation of dinitrogen.

The addition of  $[4\text{-O}_2\text{NC}_6\text{H}_4\text{N}_2][\text{BF}_4]$  or  $[4\text{-MeOC}_6\text{H}_4\text{N}_2][\text{BF}_4]$  to a solution of complex **2** in propionitrile at  $0^\circ\text{C}$  leads to a colour change from purple to brown. Evaporation of the solvent yields a brown oily solid in both cases. The reaction product was washed with hexane, giving yellow extracts. The  $^{31}\text{P}$  NMR spectrum of the oily solid indicates the presence of three diamagnetic products. The hexane extracts were subjected to a GC–MS analysis.

The hexane extract for the reaction with  $[4\text{-MeOC}_6\text{H}_4\text{N}_2][\text{BF}_4]$  contains two products stemming from a reaction of the *p*-methoxyphenyl- and the *p*-tolylthiyl functions. *p*-Methoxyphenyl *p*-tolyl sulfide ( $m/z$  230) and 1-cyano-2-(*p*-tolylthio)ethane ( $m/z$  177) were identified on the basis of their molecular-ion peaks and fragmentation pattern. The latter must be due to a reaction of the cluster radical with the solvent or a solvent radical. The extract for the reaction with  $[4\text{-O}_2\text{NC}_6\text{H}_4\text{N}_2][\text{BF}_4]$  indicates the presence of four products. Nitrobenzene ( $m/z$  123), 1-cyano-2-(*p*-tolylthio)ethane *p*-nitro-

phenyl *p*-tolyl sulfide ( $m/z$  245) and *p*-tolyl disulfide ( $m/z$  246) were identified.

In the hexane extract from the analogous reaction of the  $C_6H_4Br-4$  derivative **5** with  $[4-O_2NC_6H_4N_2][BF_4]$  it was possible to detect reaction products stemming from the coupling of the *p*-bromophenylthiyl radical and the nitrophenyl radical: nitrobenzene, 1-cyano-2-(*p*-bromophenyl)ethane ( $m/z$  241), *p*-bromophenyl *p*-nitrophenyl sulfide ( $m/z$  309), and *p*-bromophenyl disulfide ( $m/z$  374).

The results suggest that reactions of the clusters with the arenediazonium salts lead to decomposition of the cluster *via* a radical mechanism.

## Conclusion

As predicted by DFT calculations, the trinuclear  $MoCu_2$  clusters can be reduced, and for **2** oxidized reversibly, on the CV time-scale. The oxidation of **2** is shown to be molybdenum-based by EPR spectroscopy. Surprisingly, the chemical oxidation of **2** with  $NOBF_4$  leads to the formation of a diamagnetic  $MoCu_2$  cluster having a co-ordinated nitrosyl ligand. In addition to the metal-based redox chemistry, the trinuclear clusters exhibit a ligand-based redox chemistry, which leads to the decomposition of the cluster *via* a radical mechanism.

## Experimental

**General Procedures and Techniques.**—All manipulations were carried out using standard glove-box and double-manifold vacuum-line techniques under an atmosphere of dry nitrogen or argon. The salt  $NBu^n_4PF_6$  (Aldrich) was dried for 24 h at 100 °C before use and  $NBu^n_4ClO_4$  (Fluka) was recrystallized from  $Pr^iOH$ -water (70:30, v/v) and dried for 24 h in a vacuum oven at 100 °C prior to use. Dichloromethane was dried over  $P_4O_{10}$  and distilled from  $CaH_2$  prior to use, propionitrile was dried and distilled from  $CaH_2$ . Elemental analyses were performed by the University of Calgary Department of Chemistry Analytical Service Laboratory, and by the Canadian Microanalytical Services, Delta, B.C. Routine  $^1H$  NMR spectra were recorded on a Bruker ACE-200 spectrometer; a Bruker AM-400 ( $^{31}P$ ,  $^{14}N$ ) and a Varian XL-200 ( $^{31}P$ ) spectrometer were used for all other nuclei. Infrared spectra (2000–400  $cm^{-1}$ ) were recorded as KBr disks using a Mattson 4030 Galaxy Series FT-IR spectrometer, EPR data on a Varian E-12 spectrometer at X-band frequency. Frozen-solution EPR spectra were recorded at 77 K using liquid nitrogen as a coolant, with an Oxford Instruments ESR9 cryostat. The complexes  $[(Ph_3P)Cu(\mu-SR)_3Mo(\mu-SR)_3Cu(PPh_3)]$  ( $R = C_6H_4Me-4$ ,  $C_6H_4F-4$ ,  $C_6H_4Cl-4$ , or  $C_6H_4Br-4$ ),<sup>2</sup> ferrocenium hexafluorophosphate<sup>18</sup> and the diazonium salts<sup>19</sup> were synthesized according to literature procedures. The salt  $NOBF_4$  was purchased from Aldrich and used without further purification.

**Electrochemistry.**—All electrochemical experiments were carried out under an atmosphere of argon at room temperature (+20 °C). The solvent was  $CH_2Cl_2$  containing 0.1 mol  $dm^{-3}$   $NBu^n_4ClO_4$  as supporting electrolyte. The concentrations of the clusters were about 5 mmol  $dm^{-3}$ . For the cyclic voltammetry studies the working electrode was a platinum wire, positioned concentrically within the coils of a platinum-wire helix, which served as the counter electrode. The reference electrode was a saturated calomel electrode. Two fine glass frits and a Luggin capillary positioned within 2 mm of the working electrode surface separated the working and reference electrode compartments. Argon was bubbled through the solutions immediately after preparation to ensure complete removal of any traces of oxygen. The application of *IR* compensation did not change the CV data.

**EPR Sample Preparation.**—(a) *Electrochemical.* The anions  $2^-$ – $5^-$  were prepared by bulk reductive electrolysis of

complexes **2**–**5** at a platinum-wire gauze (EG + G Princeton Applied Research, Coulometric Cell System 377 A) at room temperature in a solution of 0.5 mol  $dm^{-3}$   $NBu^n_4PF_6$  in  $CH_2Cl_2$ . The specific concentrations and reduction potentials were: **2** (4.8, –1.00); **3** (2.6, –0.85); **4** (1.7, –0.70); **5** (2.6 mmol  $dm^{-3}$ , –0.70 V). The yellow-brown solutions of the reduced clusters were transferred *via* a syringe into argon-filled EPR sample tubes and immediately frozen at –196 °C. For  $2^-$ ,  $g_{\perp} = 1.921$  and  $g_{\parallel} = 1.888$ ; for  $3^-$ ,  $g_{\perp} = 1.922$  and  $g_{\parallel} = 1.891$ ; for  $4^-$ ,  $g_{\perp} = 1.921$  and  $g_{\parallel} = 1.890$ ; for  $5^-$ ,  $g_{\perp} = 1.920$  and  $g_{\parallel} = 1.887$ .

The cation  $2^+$  was prepared by bulk oxidative electrolysis at 0.49 V of a 3.7 mmol  $dm^{-3}$  solution of complex **2** in  $CH_2Cl_2$  (0.5 mol  $dm^{-3}$   $NBu^n_4PF_6$  as supporting electrolyte). The resulting brown solution was transferred *via* a syringe to an argon-filled EPR tube and immediately frozen at –196 °C. For  $2^+$ ,  $g_{\perp} = 1.984$  and  $g_{\parallel} = 1.936$ .

(b) *Chemical.* The clusters **2**–**5** (*ca.* 10 mg) and an approximately equal amount (by volume) of  $[Fe(C_3H_5)_2]PF_6$  were placed in an argon-flushed EPR sample tube. Degassed toluene-acetone (1:1 v/v) was added with a syringe. The tube was frozen immediately in liquid nitrogen. For  $2^+$ ,  $g_{\perp} = 1.984$  and  $g_{\parallel} = 1.936$ .

**Density Functional Calculations.**—The calculations were based on approximate density functional theory within the local density approximation (LDA),<sup>20</sup> extended by Becke's<sup>21</sup> non-local exchange correction and Perdew's<sup>22</sup> inhomogeneous gradient correction for correlation. The LDA potential in the parametrization of Vosko, Wilk, and Nusair (VWN)<sup>23</sup> was used self-consistently whereas Becke's correction was added as a perturbation based on the density obtained from the LDA self-consistent field (SCF) calculation. All calculations utilized the vectorized version of the AMOL program system developed by Baerends *et al.*,<sup>11</sup> and vectorized by Ravenek.<sup>24</sup> The numerical integration was based on a scheme developed by Becke.<sup>25</sup>

A double  $\xi$ -STO basis<sup>26</sup> was used for the *ns* and *np* shells of the main-group elements. For sulfur, this basis was augmented by a single 3d STO function. For hydrogen, a 2p STO was used as polarization. The *ns*, *np*, *nd*, (*n* + 1)*s* and (*n* + 1)*p* shells of molybdenum were represented by a triple  $\xi$ -STO basis. Electrons in lower shells were considered as core and treated according to the procedure of Baerends *et al.*<sup>11a</sup> A set of auxiliary<sup>27</sup> *s*, *p*, *d*, *f*, and *g* STO functions, centred on all nuclei, was used to fit the molecular density and present Coulomb and exchange potentials in each SCF cycle.

**Geometry Optimization.**—All aryl groups were represented by hydrogen atoms for ease of calculation. All calculations were done in  $D_3$  symmetry. The symmetry was maintained during the process of geometry optimization. The molecules under investigation were optimized with respect to the Mo–Cu distance, the bridging atoms and the Cu–P distance. The geometry optimization procedure was based on a method developed by Versluis and Ziegler.<sup>28</sup>

**Synthesis of  $[(Ph_3P)Cu(\mu-SC_6H_4Me-4)_3Mo(NO)(\mu-SC_6H_4Me-4)_3Cu(PPh_3)][BF_4]$ .**—The cluster  $[(Ph_3P)Cu(\mu-SC_6H_4Me-4)_3Mo(\mu-SC_6H_4Me-4)_3Cu(PPh_3)]$  (0.20 g, 0.135 mmol) was dissolved in  $CH_2Cl_2$  (20  $cm^3$ ). To the stirring purple solution  $NOBF_4$  (0.019 g, 0.160 mmol) was added. The reaction mixture was stirred at room temperature. Over a period of 15 min, a colour change from purple to brown indicated a reaction. Additional reflux of the solution for 5 min ensured completion of the reaction. Removal of the solvent *in vacuo* yielded an oily brown residue which was washed with two portions of hexane (2 × 10  $cm^3$ ) and then dried *in vacuo* for 24 h. All spectral data were for this brown oil (Found: C, 57.20; H, 4.40; N, 0.70. Calc. for  $C_{78}H_{72}BCu_2F_4MoNOP_5S_6 \cdot CH_2Cl_2$ : C, 56.20; H, 4.40; N, 0.85%). IR: 491m, 523m, 540m, 695m, 725m, 751vw, 803vs,

1016s, 1085s, 1097s, 1261s, 1436m, 1487m and 1657s  $\text{cm}^{-1}$  [ $\nu(\text{NO})$ ]. NMR:  $^1\text{H}(\text{CDCl}_3)$ ,  $\delta$  7.88–7.07 (m, 54 H) and 2.32/2.31 (18 H);  $^{31}\text{P}$  ( $\nu_3$  in Hz, %) ( $\text{CH}_2\text{Cl}_2$ ),  $\delta$  65.3 (4, 2), 46.6 (5, 5), 37.3 (4, 0.5) and 26.8 (102, 93);  $^{14}\text{N}(\text{CH}_2\text{Cl}_2)$ ,  $\delta$  10.5 ( $\text{NO}^+$ ),  $-71.7$  ( $\text{N}_2$ ), and  $-323.5$  (co-ordinated NO). UV/VIS ( $\lambda_{\text{max}}/\text{nm}$ ): 425, 475(sh), and 529(sh). Molar conductance ( $1.829 \times 10^{-3} \text{ mol dm}^{-3}$  in EtCN):  $174.4 \Omega^{-1} \text{ cm}^2 \text{ mol}^{-1}$ .

**Reactions with  $[4\text{-O}_2\text{NC}_6\text{H}_4\text{N}_2][\text{BF}_4]$ .**—Complex 2. To a stirring solution of  $[(\text{Ph}_3\text{P})\text{Cu}(\mu\text{-SC}_6\text{H}_4\text{Me-4})_3\text{Mo}(\mu\text{-SC}_6\text{H}_4\text{Me-4})_3\text{Cu}(\text{PPh}_3)]$  (0.32 g, 0.215 mmol) in EtCN ( $20 \text{ cm}^3$ ) was added freshly prepared  $[4\text{-O}_2\text{NC}_6\text{H}_4\text{N}_2][\text{BF}_4]$  (0.046 g, 0.215 mmol) at  $0^\circ\text{C}$ . The solution changed rapidly from purple to brown. The reaction mixture was allowed to stir for another 10 min. The solvent was removed *in vacuo* and the brown oily solid extracted twice with hexane ( $80 \text{ cm}^3$ ), giving a yellow hexane extract and a brown oily solid. The hexane extracts were subjected to GC–MS analysis:  $m/z$  123 ( $\text{C}_6\text{H}_5\text{NO}_2$ ), 177 ( $4\text{-CH}_3\text{C}_6\text{H}_4\text{SCH}_2\text{CH}_2\text{CN}$ ), 245 ( $4\text{-CH}_3\text{C}_6\text{H}_4\text{SC}_6\text{H}_4\text{NO}_2\text{-4}$ ), and 246 ( $4\text{-CH}_3\text{C}_6\text{H}_4\text{SSC}_6\text{H}_4\text{CH}_3\text{-4}$ ).  $^{31}\text{P}$  NMR (brown oily solid,  $\text{CDCl}_3$ ):  $\delta$  47.1, 42.1 and 27.9.

Complex 5. To a stirring solution of  $[(\text{Ph}_3\text{P})\text{Cu}(\mu\text{-SC}_6\text{H}_4\text{Br-4})_3\text{Mo}(\mu\text{-SC}_6\text{H}_4\text{Br-4})_3\text{Cu}(\text{PPh}_3)]$  (0.126 g, 0.067 mmol) in EtCN ( $10 \text{ cm}^3$ ) was added freshly prepared  $[4\text{-O}_2\text{NC}_6\text{H}_4\text{N}_2][\text{BF}_4]$  (0.016 g, 0.067 mmol) at  $0^\circ\text{C}$ . The solution changed from purple to brown within 1 min. The reaction mixture was allowed to stir for another 10 min without any noticeable colour change. The solvent was removed *in vacuo* and the resulting brown oil extracted twice with hexane ( $80 \text{ cm}^3$ ), giving a yellow hexane extract and a brown oil. The hexane extracts were subjected to GC–MS analysis:  $m/z$  123 ( $\text{C}_6\text{H}_5\text{NO}_2$ ), 241 ( $4\text{-BrC}_6\text{H}_4\text{SCH}_2\text{CH}_2\text{CN}$ ), 309 ( $4\text{-BrC}_6\text{H}_4\text{SC}_6\text{H}_4\text{NO}_2\text{-4}$ ), and 376 ( $4\text{-BrC}_6\text{H}_4\text{SSC}_6\text{H}_4\text{Br-4}$ ).

**Reaction of Complex 2 with  $[4\text{-MeOC}_6\text{H}_4\text{N}_2][\text{BF}_4]$ .**—Complex 2 (0.30 g, 0.202 mmol) was dissolved in EtCN ( $20 \text{ cm}^3$ ) and freshly prepared  $[4\text{-MeOC}_6\text{H}_4\text{N}_2][\text{BF}_4]$  (0.045 g, 0.202 mmol) was added to the stirring solution at  $0^\circ\text{C}$ . Immediately, the solution changed from purple to brown. It was stirred for another 10 min. The solvent was removed *in vacuo* and the resulting brown oil extracted with hexane ( $80 \text{ cm}^3$ ) giving a slightly yellow extract and a brown oily solid. The brown solid was dissolved in tetrahydrofuran and hexane ( $15 \text{ cm}^3$ ) added. Overnight storage at  $-20^\circ\text{C}$  produced a brown precipitate, which was washed with hexane and dried *in vacuo*. GC–MS (hexane extract):  $m/z$  230 ( $4\text{-CH}_3\text{OC}_6\text{H}_4\text{SC}_6\text{H}_4\text{CH}_3\text{-4}$ ) and 193 ( $4\text{-CH}_3\text{OC}_6\text{H}_4\text{SCH}_2\text{CH}_2\text{CN}$ ).  $^{31}\text{P}$  NMR (brown precipitate,  $\text{CDCl}_3$ ):  $\delta$  47.1, 40.6 and 27.6.

**Cross-over Experiment.**—The complexes  $[(\text{Ph}_3\text{P})\text{Cu}(\mu\text{-SC}_6\text{H}_4\text{Br-4})_3\text{Mo}(\mu\text{-SC}_6\text{H}_4\text{Br-4})_3\text{Cu}(\text{PPh}_3)]$  (0.126 g, 0.067 mmol) and  $[(\text{Ph}_3\text{P})\text{Cu}(\mu\text{-SC}_6\text{H}_4\text{Me-4})_3\text{Mo}(\mu\text{-SC}_6\text{H}_4\text{Me-4})_3\text{Cu}(\text{PPh}_3)]$  (0.100 g, 0.067 mmol) were dissolved in propionitrile ( $20 \text{ cm}^3$ ) and cooled to  $0^\circ\text{C}$ . To the stirring solution an equimolar amount of  $[4\text{-O}_2\text{NC}_6\text{H}_4\text{N}_2][\text{BF}_4]$  (0.032 g, 0.135 mmol) was added. The solution turned rapidly from purple to brown and was stirred for 10 min. The solvent was removed and the oily solid extracted with hexane. The hexane extracts were subjected to GC–MS analysis: 123 ( $\text{C}_6\text{H}_5\text{NO}_2$ ), 177 ( $4\text{-CH}_3\text{-C}_6\text{H}_4\text{SCH}_2\text{CH}_2\text{CN}$ ), 245 ( $4\text{-CH}_3\text{C}_6\text{H}_4\text{SC}_6\text{H}_4\text{NO}_2\text{-4}$ ), 246 ( $4\text{-CH}_3\text{C}_6\text{H}_4\text{SSC}_6\text{H}_4\text{CH}_3\text{-4}$ ), 309 ( $4\text{-BrC}_6\text{H}_4\text{SC}_6\text{H}_4\text{NO}_2\text{-4}$ ), 310 ( $4\text{-BrC}_6\text{H}_4\text{SSC}_6\text{H}_4\text{CH}_3\text{-4}$ ) and 376 ( $4\text{-BrC}_6\text{H}_4\text{SSC}_6\text{H}_4\text{Br-4}$ ).

### Acknowledgements

Financial support from Natural Sciences and Engineering Research Council (Canada), the Department of Chemistry for a Graduate Scholarship (to H.-B. K.) and the University of Calgary Research Services for a Thesis Research Grant (to H.-B. K.) is gratefully acknowledged. We thank Professors E. J. Baerends and W. Ravenek for a copy of their vectorized LCAO-HFS program system and the University of Calgary for access to their computing facilities. Furthermore, we thank Drs.

R. Yamdagni and I. Hunt for very helpful discussions and Qiao Wu for recording the GC–MS spectra.

### References

- J. M. Ball, P. M. Boorman, J. F. Fait and T. Ziegler, *J. Chem. Soc., Chem. Commun.*, 1989, 722.
- P. M. Boorman, H.-B. Kraatz, M. Parvez and T. Ziegler, *J. Chem. Soc., Dalton Trans.*, 1993, 433.
- R. W. Hay, *Bio-Inorganic Chemistry*, Ellis Horwood, Chichester, 1984.
- T. G. Spiro (Editor), *Molybdenum Enzymes*, Wiley, New York, 1985; R. H. Holm, *Chem. Soc. Rev.*, 1981, **10**, 455; S. J. N. Burgmayer and E. I. Stiefel, *J. Chem. Educ.*, 1985, **62**, 943; W. E. Newton, in *Sulfur, its Significance for Chemistry, for the Geo-, Bio-, and Cosmosphere*, eds. A. Müller and B. Krebs, Elsevier, Amsterdam, 1984, pp. 409–477; J. R. Dilworth in *Sulfur, its Significance for Chemistry, for the Geo-, Bio-, and Cosmosphere*, eds. A. Müller and B. Krebs, Elsevier, Amsterdam, 1984, pp. 141–265.
- D. Sellmann, B. Seubert, M. Moll and F. Knoch, *Angew. Chem., Int. Ed. Engl.*, 1988, **27**, 1164; *Z. Naturforsch., Teil B*, 1991, **46**, 1449; D. Sellmann and B. Seubert, *Angew. Chem., Int. Ed. Engl.*, 1992, **31**, 205.
- E. Block, G. Ofori-Okai, H. Kang and J. Zubietta, *J. Am. Chem. Soc.*, 1992, **114**, 758.
- L. P. Hammett, *Physikalische Organische Chemie*, Verlag Chemie, Weinheim, 1973, ch. 11, pp. 352–354.
- S. R. Ellis, D. Collison and C. D. Garner, *J. Chem. Soc., Dalton Trans.*, 1989, 413.
- B. V. DePamphilis, B. A. Averill, T. Herskovitz, L. Que and R. H. Holm, *J. Am. Chem. Soc.*, 1974, **96**, 4159.
- L. J. Lyons, M. H. Tegen, K. J. Haller, D. H. Evans and P. M. Treichel, *Organometallics*, 1988, **7**, 357.
- (a) E. J. Baerends, D. E. Ellis and P. Ros, *Chem. Phys.*, 1973, **2**, 41; (b) E. J. Baerends, Ph.D. Thesis, Frije Universiteit, Amsterdam, 1975.
- (a) P. T. Bishop, J. R. Dilworth, J. Hutchingson and J. A. Zubietta, *Inorg. Chim. Acta*, 1984, **84**, L15; (b) B. F. G. Johnson and K. H. Al-Obaidi, *Chem. Commun.*, 1968, 876.
- (a) J. Mason, *Chem. Rev.*, 1981, **81**, 205; (b) R. E. Botto, B. W. S. Kolthammer, P. Legzdins and J. D. Roberts, *Inorg. Chem.*, 1979, **18**, 2049; (c) L. K. Bell, D. M. P. Mingos, D. G. Tew, L. F. Larkworthy, B. Sandell, D. C. Povey and J. Mason, *J. Chem. Soc., Chem. Commun.*, 1983, 125; (d) R. E. Stevens and W. L. Gladfelter, *Inorg. Chem.*, 1983, **22**, 2034; (e) L. K. Bell, J. Mason, D. M. P. Mingos and D. G. Tew, *Inorg. Chem.*, 1983, **22**, 3497; (f) D. H. Evans, D. M. P. Mingos, J. Mason and A. Richards, *J. Organomet. Chem.*, 1983, **249**, 293.
- (a) J. H. Enemark and R. D. Feltham, *Coord. Chem. Rev.*, 1974, **13**, 339; (b) D. M. P. Mingos, *Inorg. Chem.*, 1973, **12**, 1209; (c) R. Hoffmann, M. M. L. Chen, M. Elian, A. R. Rossi and D. M. P. Mingos, *Inorg. Chem.*, 1974, **13**, 2666; (d) D. M. P. Mingos and D. J. Sherman, *Adv. Inorg. Chem.*, 1989, **34**, 293.
- See K. Nakamoto, *Infrared Spectra of Inorganic and Coordination Compounds*, Wiley, New York, 1963, p. 106.
- A. J. Fry, in *The Chemistry of Diazonium and Diazo Groups*, ed. S. Patai, Wiley, Chichester, 1978, ch. 10, pp. 496–498.
- J. March, *Advanced Organic Chemistry*, McGraw-Hill, Tokyo, 1984, ch. 14, pp. 659–663.
- D. N. Hendrickson, Y. S. Sohn and H. B. Gray, *Inorg. Chem.*, 1971, **10**, 1559.
- E. B. Starkey, in *Organic Syntheses Collective Volume 2*, ed. A. H. Blatt, Wiley, New York, 1969, pp. 225–227.
- O. Gunnarsson and I. Lundquist, *Phys. Rev. B*, 1974, **10**, 1319; 1976, **13**, 4274; O. Gunnarsson, M. Johnson and I. Lundquist, *Phys. Rev. B*, 1979, **20**, 3136.
- A. Becke, *J. Phys. Chem.*, 1986, **84**, 4524; 1988, **88**, 1053.
- J. P. Perdew, *Phys. Rev. B*, 1986, **33**, 8822; **34**, 7406 (erratum).
- S. H. Vosko, L. Wilk and M. Nusair, *Can. J. Phys.*, 1980, **88**, 2547.
- W. Ravenek, in *Algorithms and Applications on Vector and Parallel Computers*, eds. H. J. J. Riele, Th. J. Dekker and H. A. van de Horst, Elsevier, Amsterdam, 1987.
- A. Becke, *J. Chem. Phys.*, 1988, **88**, 2547.
- J. G. Snijders, E. J. Baerends and P. Vernooijs, *At. Data Nucl. Data Tables*, 1982, **26**, 483; P. Vernooijs, J. G. Snijders and E. J. Baerends, *Slater Type Basis Functions for the Whole Periodic System, Internal Report*, Frije Universiteit, Amsterdam, 1981.
- J. Krijn and E. J. Baerends, *Fitfunctions in the HFS method, Internal Report*, Frije Universiteit, Amsterdam, 1984.
- L. Versluis and T. Ziegler, *J. Chem. Phys.*, 1988, **88**, 322.

Received 30th October 1992; Paper 2/05813H